On the Survivable Multilayer Planning of Filterless Optical Networks with P2MP Transceivers

Qian Lv, Ruoxing Li, and Zuqing Zhu, *Fellow, IEEE*

***Abstract*—The rapid development of emerging network services are shifting the major communication scheme in metro-aggregation networks from unicast to in-cast and multicast, which has promoted the development of the point-to-multipoint coherent optical transceivers (P2MP-TRXs). Meanwhile, for its cost-effectiveness and energy-efficiency, filterless optical network (FON) has been considered as a promising optical infrastructure for metro-aggregation networks, and it is naturally compatible with P2MP-TRXs because they both rely on the broadcast-and-select scheme for communications. In this paper, we study the problem of survivable multilayer planning of FONs with P2MP-TRXs and design algorithms to ensure that the planned FON can protect itself against single-link failures. We first formulate a mixed integer linear programming (MILP) model to jointly optimize the routing of working and backup lightpaths of traffic demands, and the allocation of P2MP-TRXs, assignment of subcarriers (SCs) to P2MP-TRXs, spectrum assignment on fiber trees for setting up the lightpaths, such that the capital expenditures (CAPEX) of the planned FON is minimized. Then, to solve the problem more time-efficiently, we propose a polynomial-time heuristic based on auxiliary graphs (AGs) and lightpath grouping. Extensive simulations verify the performance of our proposals and indicate that they can outperform existing benchmarks.**

***Index Terms*—Filterless optical networks, Point-to-multipoint transceivers, Survivable multilayer network planning.**

I. Introduction

NOWADAYS, the Internet is under rapid development to adapt to the explosion of emerging network services, and the rising of 5G communications, cloud computing and data-center networks (DCNs) has put great pressure on the underlying infrastructure of the Internet, *i.e.*, fiber optic networks, especially for the metro segments [1–3]. Therefore, network operators are continuously looking for more cost-effective optical networking technologies to improve flexibility while reducing capital expenditures (CAPEX) and operating expenses (OPEX). For instance, flexible-grid elastic optical networking (EON) was proposed and has attracted intensive interest in the past decade [4–10], as it can make the resource allocation in the optical layer much more adaptive and effectively improve the spectrum efficiency of data transmissions.

Although previous advances on optical networking technologies did greatly improve the cost-effectiveness of the Internet, the ever-growing network services have been generating new challenges constantly. For example, cloud computing and DCNs have brought in large amounts of in-cast and multicast traffic, and shifted the major communication schemes in metro-aggregation networks from point-to-point (P2P) to hub&spoke (H&S) [11–13]. This has promoted the development of the point-to-multipoint (P2MP) coherent optical transceivers (P2MP-TRXs) [14]. Specifically, one set of P2MP-TRXs can realize in-cast and multicast in the upstream and downstream directions, respectively, and thus the optical infrastructure can be effectively simplified, saving both CAPEX and OPEX [13].

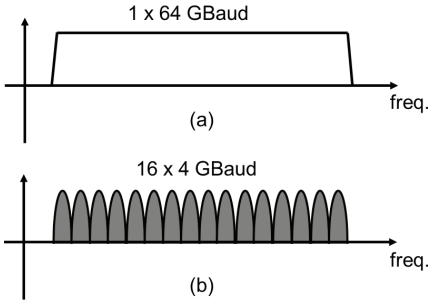

Fig. 1. Realizing 400 Gbps capacity with (a) a single carrier and (b) DSCM.

With digital subcarrier multiplexing (DSCM), P2MP-TRXs can slice the capacity of an optical channel adaptively and enable a single high-rate transceiver (TRX) (*i.e.*, the hub node) to communicate with multiple low-rate TRXs (*i.e.*, the leaf nodes) [14]. In a P2MP-TRX, the data transmission is realized with a set of digital subcarriers (SCs), which do not overlap in the spectrum domain and can be independently modulated, grouped, and routed to different destinations [15]. Hence, P2MP-TRXs further reduce the bandwidth allocation granularity in the optical layer, while maintaining the complexity and cost of a P2MP-TRX similar to those of a conventional P2P-TRX that operates at the same maximum line-rate [16].

Fig. 1 illustrates the difference between realizing the same transmission capacity with a single carrier and DSCM. Specifically, in order to deliver a capacity of 400 Gbps, one can leverage a single-carrier scheme with dual-polarization and 16 quadrature amplitude modulation (DP-16QAM), which occupies 64 GHz spectrum, and with the same spectrum occupancy, he/she can also use a DSCM scheme with 16 SCs, each of which occupies 4 GHz to achieve a capacity of 25 Gbps with DP-16QAM. Therefore, with the DSCM scheme in Fig. 1, one 400-Gbps P2MP-TRX at a hub node can easily establish four 25-Gbps connections respectively with four 100-Gbps TRXs at leaf nodes, as long as the TRXs at leaf nodes have been tuned to the right SCs. Note that, the connections among the hub and leaf nodes can even be realized without any wavelength-switching components in between, *i.e.*, by using

Q. Lv, R. Li, and Z. Zhu are with the School of Information Science and Technology, University of Science and Technology of China, Hefei, Anhui 230027, P. R. China (email: zqzhu@ieee.org).

Manuscript received on November 3, 2022.

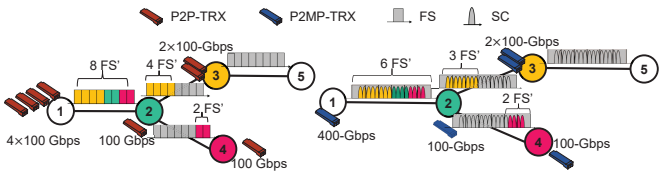

Demand	Rate (Gbps)	Modulation	Assigned SCs to P2MP-TRXs
1-4	100	DP-16QAM	4
1-2	100	DP-16QAM	4
1-3	200	DP-16QAM	8

(c)

Fig. 2. Example on building an FON with P2P-TRXs and P2MP-TRXs.

passive optical splitters/combiners [14].

The operation principle of P2MP-TRXs makes them a good match for being implemented in filterless optical networks (FONs) [17]. Specifically, FON replaces wavelength switching elements in wavelength-division multiplexing (WDM) networks with passive optical splitters/combiners, and thus can improve the cost-effectiveness and energy-efficiency of the optical layer [18]. Without wavelength switching elements, FON lets the WDM signal enters each of its nodes be broadcasted to all of the node's downstream neighbors, and counts on the TRXs located at the actual destinations to select the desired WDM channels, *i.e.*, using the "broadcast-and-select" scheme. Hence, to design one FON with a mesh topology, one first needs to partition the topology into a few loopless fiber trees to avoid causing laser-loops due to continuous signal broadcasting and amplification [18], and meanwhile, there will be redundant spectrum consumption on the fiber trees because of the broadcast-and-select scheme. Moreover, as FONs are based on fiber trees, they are naturally more suitable for carrying H&S traffic in aggregation-metro networks, saving CAPEX and OPEX more effectively [19, 20]. Therefore, building FONs with P2MP-TRXs will be promising.

Apart from the fact that FONs and P2MP-TRXs are naturally compatible because they both use the broadcast-and-select scheme, the absence of wavelength switching elements in FONs makes the data transmissions with P2MP-TRXs much easier, *i.e.*, avoiding the hassle of SC-level optical filtering. Fig. 2 provides an illustrative example to explain the benefits that P2MP-TRXs achieve in FONs over P2P-TRXs. The FON only consists of one fiber tree that connects five nodes, and the traffic demands are listed in the table in Fig. 2, *i.e.*, two 100-Gbps demands from *Node* 1 to *Nodes* 2 and 4, respectively, and one 200-Gbps demand from *Node* 1 to *Node* 3. The P2P-TRXs and P2MP-TRXs all use DP-16QAM as their modulation format. Hence, if the FON is built with P2P-TRXs (as shown in Fig. 2(a)), we need to allocate one 100-Gbps P2P-TRX on each of *Nodes* 1 and 4 for the first demand, and so on so forth. The data transmission between each pair of 100-Gbps P2P-TRXs occupies a bandwidth of 25 GHz (*i.e.*, two 12.5-GHz frequency slots (FS')). This makes the FON use eight 100-Gbps P2P-TRXs on nodes and 32 FS' on links, where 18 FS' are wasted due to the broadcast-and-select scheme.

On the other hand, if we architect the FON with P2MP-TRXs, only one 400-Gbps hub P2MP-TRX needs to be placed on *Node* 1, which respectively works with four 100-Gbps leaf P2MP-TRXs. We assume that each SC of a P2MP-TRX occupies 4 GHz and delivers a capacity of 25 Gbps, and then the first two demands can be supported with 4 SCs and the last one will need 8 SCs. Therefore, the total bandwidth used by the 400-Gbps hub P2MP-TRX is $16 \times 4 = 64$ GHz, which can be accommodated by six 12.5-GHz FS' since the SCs and FS' do not need to use the same central frequency [21]. Then, the spectrum assignment in the FON becomes that in Fig. 2(b), which uses 24 FS' on links, wasting 13 FS' in total[1]. Hence, P2MP-TRXs not only simplify the FON's configuration but also reduce redundant spectrum usage in it.

Note that, for an FON that consists of multiple fiber trees, its network planning to serve a set of traffic demands has to be a multilayer one. This is because certain source-destination pairs are not connected in the optical layer as none of the fiber trees can cover all the nodes [22]. Therefore, the network planning needs to consider the traffic grooming/degrooming at the edge of fiber trees. However, to the best of our knowledge, the comprehensive version of multilayer planning of FONs with P2MP-TRXs, which needs to jointly optimize the allocation of P2MP-TRXs, the assignment of SCs to P2MP-TRXs, the spectrum assignment on fiber trees, and the routing of traffic demands, has not been studied in the literature yet. Note that, although spectrum saving could be less important in FONs, designing efficient spectrum assignment schemes to avoid spectrum waste is still meaningful. This is because spectrum usage also contributes to CAPEX [23–25]. Meanwhile, a practical planning should not overlook network survivability, as fatal failures such as fiber cuts and node failures can happen everywhere and severely impact network services [26]. Moreover, the damage caused by these failures can even be amplified when network virtualization [27–29] is in place, *i.e.*, the failure of a physical device can interrupt the services of all the virtual networks that share it [30]. Nevertheless, due to its complexity, the problem of survivable multilayer planning of FONs with P2MP-TRXs will be much more challenging.

In this work, we study the problem of survivable multilayer planning of FONs with P2MP-TRXs and design algorithms to ensure the protection against single-link failures. We first formulate a mixed integer linear programming (MILP) model to jointly optimize the allocation of P2MP-TRXs, the assignment of SCs to P2MP-TRXs, the spectrum assignment on fiber trees, and the working and backup routing of traffic demands, such that the CAPEX of the planned FON is minimized. To the best of our knowledge, such a comprehensive version of survivable multilayer planning of FONs with P2MP-TRXs has not been studied in the literature yet. Then, to accelerate the problem-solving, we design a time-efficient heuristic based on auxiliary graphs (AGs). Extensive simulations verify the performance of our proposed algorithms and suggest that they can significantly outperform the existing scheme designed in [31], which, to the best of our knowledge, is the only known algorithm that tackles survivable planning of FONs with P2MP-TRXs.

[1]Here, the spectra received by the leaf P2MP-TRXs on *Nodes* 2, 3 and 4 are 2, 3 and 2 FS', respectively, whose sum is more than the 6 FS' from the hub P2MP-TRX on *Node* 1. This is because there are mismatches between SCs and FS', and thus SCs to different leaf P2MP-TRXs can share an FS.

The rest of this paper is organized as follows. Section II surveys the related work. The problem description and MILP model of the survivable multilayer planning of FONs with P2MP-TRXs are presented in Section III. Then, we propose our heuristic algorithm in Section IV, and the performance evaluations with simulations are discussed in Section V. Finally, Section VI summarizes the paper.

II. Related Work

Recently, there have been intensive studies on DSCM-based P2MP-TRXs, and people have demonstrated their performance in both lab environments [32] and field trials [33]. Meanwhile, the techno-economic advantages of P2MP-TRXs over conventional P2P-TRXs have been analyzed in [34, 35]. The studies in [13, 36] have commented on the structural compatibility of P2MP-TRXs and FONs, and discussed how to build FONs with P2MP-TRXs. On the other hand, the network planning and service provisioning of FONs have been considered in [23–25, 37, 38]. They suggested that the establishment of fiber trees, the spectrum assignment on fiber trees, and the routing of traffic demands are the key factors for minimizing the redundant spectrum consumption in an FON, where the establishment of fiber trees limits the solution space of the remaining two factors. Therefore, the studies in [24, 37, 38] assumed pre-established fiber trees[2] and solved the optimization of the remaining two factors, while the authors of [23, 25] tried to jointly optimize all the three factors. Xu *et al.* [39] addressed the survivability of FONs, and tried to protect FONs against single-link failures with "1+1" dedicated path protection (DPP). However, as the studies in [23–25, 37–39] were all based on P2P-TRXs and did not consider P2MP-TRXs, their proposals can hardly be leveraged to address the problem considered in this work.

In order to plan an FON with P2MP-TRXs, one needs to determine the allocation of P2MP-TRXs, the assignment of SCs to P2MP-TRXs, the spectrum assignment on fiber trees, and the routing of traffic demands, and the designed algorithm should be generic enough to handle mesh topologies. In [13], the authors studied the planning of FONs with P2MP-TRXs and confirmed that the planned FONs would be more cost-effective than those with P2P-TRXs. Nevertheless, the study only addressed horseshoe topologies and did not optimize SC and spectrum assignments. Assuming ring topologies, Pavon-Marino *et al.* [21] proposed algorithms to jointly optimize the allocation of P2MP-TRXs, the assignment of SCs to P2MP-TRXs, and the routing of traffic demands.

The study in [40] addressed the planning of mesh FONs with P2MP-TRXs for metro-aggregation networks, but did not optimize the spectrum assignment on fiber trees. Later, in its follow-up work [31], survivable FON planning with P2MP-TRXs was considered. However, the algorithm designed in [31] still has a few limitations. First, it proposed to find two link-disjoint spanning trees in the physical topology of an FON as the working and backup fiber trees to protect against single-link failures. This, however, applies restrictions on the physical topology because it might not be feasible to obtain two link-disjoint spanning trees in an arbitrary mesh topology. Second, since the algorithm tried to cover an FON with a single fiber tree, it might have difficulty to adapt to various traffic patterns other than the H&S ones and did not consider the multilayer planning that needs to address traffic grooming/degrooming between fiber trees. This makes the algorithm less generic. Third, as it just assigned separate P2MP-TRXs to the working and backup fiber trees, the P2MP-TRXs might not be utilized efficiently. Last but most importantly, it still did not optimize the spectrum assignment on fiber trees, and thus did not address survivable FON planning in the comprehensive manner.

Hence, to the best of our knowledge, the comprehensive version of survivable multilayer planning of FONs with P2MP-TRXs, which involves the joint optimization of the allocation of P2MP-TRXs, the assignment of SCs to P2MP-TRXs, the spectrum assignment on fiber trees, and the working and backup routing of traffic demands, has not been studied yet.

[2]The fiber trees in an FON have been determined before the network planning and remain unchanged during network operation.

III. Problem Description

This section first describes the network model of survivable multilayer planning of FONs with P2MP-TRXs, and then formulates an MILP model to define the optimization problem.

A. Network Model

We model an FON's physical topology (*i.e.*, the mesh layout of its fiber connections) as a graph $G(V, E)$, where V represents the set of nodes and E is the set of directional fiber links. Each $v \in V$ denotes a filterless optical node, which is built with passive splitters/combiners and P2MP-TRXs. This work considers two types of P2MP-TRXs, *i.e.*, the hub and leaf P2MP-TRXs [14]. For simplicity, we assume that each leaf P2MP-TRX can only connect to a hub, and operates at a lower data-rate by only processing the SCs assigned to it. According to the settings described in [14], we set the feasible capacities of P2MP-TRXs as $\{25, 100, 400\}$ Gbps, and assume that each SC uses DP-16QAM at 4 GBaud to realize a capacity of 25 Gbps. Therefore, the number of SCs to realize overall capacities of $\{25, 100, 400\}$ Gbps are $\{1, 4, 16\}$, respectively, and their spectrum usages respectively become $\{1, 2, 6\}$ FS', where each FS occupies 12.5 GHz.

To reduce the complexity of the survivable multilayer planning, we assume that the fiber trees in the FON have been pre-established, similar to the studies in [24, 37, 38]. Within each fiber tree, data transmissions use the broadcast-and-select scheme, and if the source and destination of a traffic demand reside in different fiber trees, its data transmission needs to be relayed by P2MP-TRXs at the edge of related fiber trees. The survivable multilayer planning needs to design an FON with P2MP-TRXs for serving a set of traffic demands $\mathcal{R}$. Each demand is modeled as $r(s_r, d_r, b_r) \in \mathcal{R}$, where s_r and d_r are its source and destination nodes, respectively, and b_r is the data-rate in number of required SCs, where each SC delivers a capacity of 25 Gbps. To serve the demands in $\mathcal{R}$, we need to place P2MP-TRXs on the nodes in V to carry their data transmissions, assign SCs to the P2MP-TRXs to ensure sufficient capacities, and allocate FS' on the links of each fiber

tree to route each demand correctly. Moreover, to ensure that the service to each demand is intact during any single-link failure, we have to plan two link-disjoint routing paths for it (*i.e.*, the working and back paths), by leveraging DPP [39].

Fig. 3 gives an example on the survivable multilayer planning of FONs with P2MP-TRXs. As shown in Fig. 3(a), the FON consists of two pre-established fiber trees, whose links are marked in blue and black, respectively. Specifically, the tree in blue (*i.e.*, *Tree* 1) covers *Nodes* $\{1, 2, 3, 4, 6\}$ with *Links* $\{1\text{-}2, 2\text{-}3, 2\text{-}4, 4\text{-}6\}$, while the one in black (*i.e.*, *Tree* 2) consists of *Nodes* $\{1, 3, 4, 5, 6\}$ and *Links* $\{1\text{-}3, 3\text{-}5, 4\text{-}5, 5\text{-}6\}$. The table in Fig. 3(a) lists the demands. Fig. 3(b) shows the allocation of P2MP-TRXs and SCs and working and backup paths of each demand. Here, we use H^a to denote a hub P2MP-TRX a, while a leaf P2MP-TRX b that connects to it is labeled as L_b^a, each set of hub/leaf P2MP-TRXs is identified by a color. Note that, each P2MP-TRX only works as either a hub or a leaf but transmits/receives signals simultaneously. We also distinguish the SCs assigned to the demands as red, purple, and yellow for r_1, r_2, and r_3, respectively.

As for r_1, the network planning in Fig. 3(b) indicates that its working path is 1-3 in *Tree* 2, which is protected by the backup path 1-2-3 in *Tree* 1. Since the working and backup paths of r_1 are respectively routed in single fiber trees, we assign it to use hub P2MP-TRX H^1 on its source (*Node* 1), and place a leaf P2MP-TRX L_1^1 on its destination (*Node* 3). Meanwhile, as 1+1 DPP is used and the data-rate of r_1 is 125 Gbps, we need to allocate 5 SCs for the working and backup paths of r_1, respectively, as shown in Fig. 3(b), *i.e.*, r_1 consumes 10 SCs on hub P2MP-TRX H^1 and leaf P2MP-TRXs L_1^1.

The working path of r_2 is 1-3-5, which is only routed in *Tree* 2. However, its backup path cannot be routed in a single fiber tree, and takes 1-2-4 in *Tree* 1 and 4-5 in *Tree* 2. This means that the backup path of r_2 is relayed on *Node* 4. Hence, as shown in Fig. 3(b), r_2 occupies 4 SCs on H^1 on *Node* 1 (for working and backup paths), 2 SCs on L_2^1 on *Node* 5 (for working path), and 2 SCs on L_3^1 on *Node* 4, one SC on each of L_2^2 and L_3^2 on *Node* 4, and 2 SCs on H^2 on *Node* 5 (for backup path). In Fig. 3(b), both the working and backup paths of r_3 are routed across two fiber trees. Therefore, r_3 occupies 6 SCs on H^2 on *Node* 5, 3 SCs on each of L_2^2 and L_1^4 on *Node* 4, 3 SCs on each of L_1^3 and L_1^2 on *Node* 3, and 3 SCs on each of H^3 and H^4 on *Node* 2. In summary, the three demands use four sets of P2MP-TRXs, where r_1 and r_2 share H^1 on *Node* 1, and r_2 and r_3 share H^2 on *Node* 5 and L_2^2 on *Node* 4.

After placing P2MP-TRXs and allocating SCs on them to demands, we need to determine the spectrum assignment on fiber trees to complete the network planning. In this work, we assume that each demand $r(s_r, d_r, b_r)$ requires symmetric capacities for $s_r \rightarrow d_r$ and $d_r \rightarrow s_r$. Hence, we only need to plan the FON to accommodate the demands in one direction, while their capacities in the reverse direction can be easily supported with a symmetric configuration. Similar to that in EONs [4], the spectrum assignment on fiber trees needs to satisfy the spectrum contiguity and non-overlapping constraints. Specifically, the FS' assigned to carry the optical signal from each P2MP-TRX should be contiguous in the spectrum domain, due to the working principle of DSCM [14]. Meanwhile, for each P2MP-TRX, its assigned FS' need to cover the spectrum of the used SCs, thus its FS assignment depends on the SCs assigned to it and the FS usage on the corresponding routing path(s). Hence, as there are 14 used SCs from H^1 with a spectrum of 56 GHz, we need to assign 5 FS' on each link of *Trees* 1 and 2, due to the broadcast-and-select scheme. Similarly, we assign 3 FS' on each link of *Tree* 2, 1 FS on each link of *Tree* 1, and 1 FS on each link of *Tree* 1, to accommodate the used SCs on H^2, H^3, and H^4, respectively, as shown in Fig. 3(c).

B. MILP Model

The following MILP models the optimization problem of survivable multilayer planning of FONs with P2MP-TRXs.

Parameters:

- $\mathcal{R}$: the set of traffic demands to serve in the network planning, where each demand r is denoted as $r(s_r, d_r, b_r)$.
- $G(V, E)$: the physical topology of the FON, where V and E are the sets of nodes and fiber links, respectively.
- $G'(V_k, E_k, P_k)$: the topology of the k-th fiber tree in the FON, where V_k, E_k, P_k are the node set, link set, path set in the fiber tree. There are K fiber trees in total.
- n_k: the number of fiber links in the k-th fiber tree.
- $f^k_{(u,v),(u',v')}$: the boolean that equals 1 if paths for u-v and u'-v' (*i.e.*, (u, v) and (u', v')) are on the k-th fiber tree and they share at least one link, and 0 otherwise.
- T: the maximum number of P2MP-TRXs that can be placed on each node $v \in V$, where $t \in [1, T]$ indicates the t-th available P2MP-TRX.
- C_t: the cost of the t-th available P2MP-TRX.
- S: the unit cost of using an FS.
- I^m: the maximum number of SCs that can be used by any P2MP-TRX.
- I_t: the maximum number of SCs that can be used by the t-th P2MP-TRX on a node.
- F: the maximum number of FS' that can be accommodated by a fiber link.
- N: a big arithmetic number.

Variables:

- $Z^r_{(u,v),k}$: the boolean variable that equals 1 if a demand $r \in \mathcal{R}$ needs to be relayed/received after going through a path (u, v) in the k-th fiber tree, and 0 otherwise.
- $M^{v,t,k}_{u,p}$: the integer variable that indicates the number of SCs assigned between the t-th P2MP-TRX on node v (leaf) and the p-th P2MP-TRX on node u (hub), and these two P2MP-TRXs serve demand(s) in the k-th fiber tree.
- $m^{v,t}_{u,p}$: the boolean variable that equals 1 if the t-th P2MP-TRX on node v and the p-th P2MP-TRX on node u are used as a leaf P2MP-TRX and its hub, and 0 otherwise.
- $H^k_{u,p}$: the boolean variable that equals 1 if the p-th P2MP-TRX on node u is allocated as a hub and its output is broadcasted in the k-th fiber tree, and 0 otherwise.
- $s_{v,t}$: the boolean variable that equals 1 if the t-th P2MP-TRX on node v is used, and 0 otherwise.
- $w^1_{v,t}/w^2_{v,t}$: the integer variable that indicates the first/last FS assigned to the t-th P2MP-TRX on node v.
- $\alpha^{v,t}_{u,p}$: the boolean variable that equals 1 if the first FS used by the t-th P2MP-TRX on node v is smaller than that used

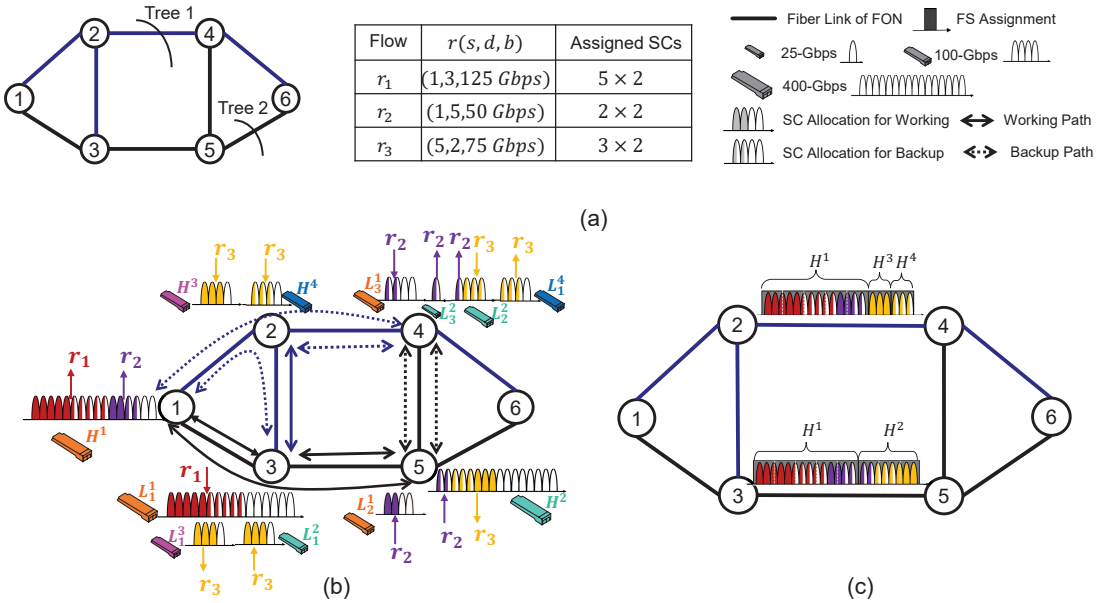

Fig. 3. Example on survivable multilayer planning of an FON with P2MP-TRXs, (a) Physical topology, fiber trees, and traffic demands, (b) Allocation of P2MP-TRXs and SCs, and working and backup routing of demands, and (c) Assignment of FS' on links in fiber trees.

by the p-th P2MP-TRX on node u, and 0 otherwise.

- $\phi_{v,t,u,p}$: the boolean variable that equals 1 if the t-th P2MP-TRX on node v and the p-th P2MP-TRX on node u are hubs and their outputs are broadcasted to at least one common fiber tree, and 0 otherwise.
- $\psi^k_{u,p}$: the integer variable for the number FS' used by the p-th P2MP-TRX (a hub) on node u in the k-th fiber tree.
- $\eta^k_{v,t,u,p}$: the auxiliary boolean variables that are introduced for linearization.

Objective:

The optimization objective of the survivable multilayer planning is to minimize the CAPEX, which is the total cost of the P2MP-TRXs and FS' used in the FON.

$$\text{Minimize} \sum_{v\in V, t\in[1,T]} \left(2\cdot \sum_{k\in[1,K]} \psi^k_{v,t}\cdot n_k \cdot S + C_t \cdot s_{v,t} \right). \quad (1)$$

Constraints:

1) Constraints for routing demands:

$$\sum_k \left(\sum_{(u,v)\in P_k} Z^r_{(u,v),k} - \sum_{(v,u)\in P_k} Z^r_{(v,u),k} \right) = \begin{cases} 2, & u = s_r, \\ -2, & u = d_r, \\ 0, & \text{otherwise}, \end{cases} \quad \forall r\in\mathcal{R}, u\in V, \quad (2)$$

$$Z^r_{(u,v),k} + Z^r_{(u',v'),k} \le \left(1 - f^k_{(u,v),(u',v')}\right)\cdot N + 1, \quad \forall r,\ k,\ (u,v),(u',v')\in P_k. \quad (3)$$

Eqs. (2)-(3) ensure that the working and backup paths of each demand are set correctly, where Eq. (2) routes the working and backup paths for each demand and Eq. (3) ensures that its working and backup paths are link-disjoint.

2) Constraints for allocating P2MP-TRXs and SCs:

$$\sum_r b_r \cdot \left(Z^r_{(u,v),k} + Z^r_{(v,u),k}\right) \le \sum_{t,p} \left(M^{v,t,k}_{u,p} + M^{u,p,k}_{v,t} \right), \quad \forall k,(u,v)\in P_k. \quad (4)$$

Eq. (4) ensures that the data-rate of each demand is satisfied.

$$M^{v,t,k}_{u,p} \le \min\{I_t, I_p\}, \quad \forall\ k,(u,v)\in P_k,\ t,p\in[1,T], \quad (5)$$

$$\sum_{v,t,k} M^{v,t,k}_{u,p} \le I_p, \quad \forall u\in V,\ p\in[1,T]. \quad (6)$$

Eqs. (5)-(6) ensure that the assignment of SCs is set correctly on each P2MP-TRX, where Eq. (5) limits the number of SCs assigned to a P2MP-TRX within the upper limit and Eq. (6) ensures that the total number of SCs assigned to leaf P2MP-TRXs cannot exceed that assigned to their hub P2MP-TRX.

$$M^{v,t,k}_{u,p} \le N\cdot m^{v,t}_{u,p},\ \forall k,(u,v)\in P_k,\ t,p\in[1,T], \quad (7)$$

$$m^{v,t}_{u,p} + \sum_{u'\in V, p'\in[1,T]} m^{u,p}_{u',p'} \le 1,\ \forall v,u\in V,\ t,p\in[1,T]. \quad (8)$$

Eqs. (7)-(8) ensure that the mapping between each hub P2MP-TRX and its leaf P2MP-TRXs is determined correctly, where Eq. (7) sets variables $\{m^{v,t}_{u,p}\}$ correctly and Eq. (8) ensures that each leaf P2MP-TRX can only connect to a hub P2MP-TRX, and one P2MP-TRX works as either a hub or a leaf only.

$$M^{v,t,k}_{u,p} \le N\cdot H^k_{u,p},\ \forall v,u\in V,\ p,t\in[1,T],k, \quad (9)$$

$$N\cdot\phi_{v,t,u,p} \ge \sum_k \left(H^k_{u,p}\cdot H^k_{v,t} \right),\ \forall v,u\in V,\ t,p\in[1,T]. \quad (10)$$

Eqs. (9)-(10) ensure that variables $\{\phi_{v,t,u,p}\}$ are set correctly, where Eq. (9) sets variables $\{H^k_{u,p}\}$ correctly and Eq. (10) sets variables $\{\phi_{v,t,u,p}\}$ correctly based on $\{H^k_{u,p}\}$.

$$\begin{cases} \eta^k_{v,t,u,p} \le H^k_{u,p}, \\ \eta^k_{v,t,u,p} \le H^k_{v,t}, \\ \eta^k_{v,t,u,p} \ge H^k_{u,p} + H^k_{v,t} - 1, \end{cases} \quad \forall t,p\in[1,T],\ v,u,\ k, \quad (11)$$

$$N \cdot \phi_{v,t,u,p} \geq \sum_{k} \eta^{k}_{v,t,u,p},\ \forall v,u \in V,\ t,p \in [1,T]. \tag{12}$$

Eqs. (11)-(12) linearize the nonlinear constraint in Eq. (10).

$$s_{v,t} \geq m^{v,t}_{u,p}, \quad \forall u,v,\ t,p, \tag{13}$$

$$s_{u,p} \geq m^{v,t}_{u,p}, \quad \forall u,v,\ t,p. \tag{14}$$

Eqs. (13)-(14) determine the used P2MP-TRXs.

3) Constraints for assigning FS' on fiber trees:

$$4 \cdot \sum_{v,t,k} M^{v,t,k}_{u,p} \leq 12.5 \cdot \left(w^{2}_{u,p} - w^{1}_{u,p} + 1\right), \quad \forall u,\ p. \tag{15}$$

Eq. (15) ensures that enough FS' are assigned to support the spectrum requirement of each P2MP-TRX.

$$\alpha^{u,p}_{v,t} + \alpha^{v,t}_{u,p} = 1, \quad \{u,v \in V,\ t,p \in [1,T] : u \neq v \text{ or } p \neq t\}, \tag{16}$$

$$w^{2}_{v,t} - w^{1}_{u,p} + 1 \leq F \cdot \left(1 + \alpha^{u,p}_{v,t} - \phi^{v,t}_{u,p}\right),\ \forall t,p \in [1,T],\ u,v, \tag{17}$$

$$w^{2}_{v,t} \leq F, \quad \forall v,\ t. \tag{18}$$

Eqs. (16)-(18) ensure that the FS' assigned to P2MP-TRXs satisfy the spectrum non-overlapping constraint.

$$\psi^{k}_{v,t} = H^{k}_{v,t} \cdot \left(w^{2}_{v,t} - w^{1}_{v,t} + 1\right), \quad \forall k,\ v,\ t. \tag{19}$$

Eq. (19) determines the FS' assigned to each hub P2MP-TRX.

$$\begin{cases} \psi^{k}_{v,t} \leq I^{m} \cdot H^{k}_{v,t}, \\ \psi^{k}_{v,t} \leq w^{2}_{v,t} - w^{1}_{v,t} + 1, \\ \psi^{k}_{v,t} \geq \left(w^{2}_{v,t} - w^{1}_{v,t} + 1\right) - I^{m} \cdot \left(1 - H^{k}_{v,t}\right), \end{cases} \quad \forall k,\ v,\ t. \tag{20}$$

Eq. (20) linearizes the nonlinear constraint in Eq. (19).

IV. Heuristic Algorithm Design

Although the MILP above can obtain the optimal solution of survivable multilayer planning of FONs with P2MP-TRXs, its complexity can make the problem-solving time-consuming or even intractable, especially for large-scale network instances. Therefore, in this section, we propose a polynomial-time heuristic, namely, AG-LPG, for near-optimal network planning solutions. We also present a heuristic (*i.e.*, AG-GRD) as the benchmark to validate the effectiveness of AG-LPG.

A. Algorithm Design

In the following, we design two polynomial-time heuristics to solve the survivable multilayer planning of FONs with P2MP-TRXs. The first algorithm (AG-LPG) uses an auxiliary graph (AG) based approach to find working and protection lightpaths (LPs) and group the LPs to adapt to the operation principle of P2MP-TRXs for better cost-effectiveness. The second one is the benchmark (AG-GRD), which also leverages the AG-based approach to find working and protection LPs but does not group LPs (*i.e.*, just setting up the LPs greedily in a sorted order to utilize P2MP-TRXs to the maximum extent).

The overall procedure of AG-LPG is shown in *Algorithm* 1, which utilizes two sub-procedures (*Algorithms* 2 and 3) to realize survivable multilayer planning of FONs with P2MP-TRXs. Specifically, *Algorithm* 1 first uses an AG-based approach to calculate the working and backup LPs for each traffic demand in $\mathcal{R}$, and then leverages *Algorithm* 2 to group LPs and assign P2MP-TRXs and spectra to them accordingly, where the assignments of P2MP-TRXs and spectra are obtained with *Algorithm* 3 (*i.e.*, a sub-procedure of *Algorithm* 2).

Algorithm 1 greedily determines the working and backup LPs of each demand $r \in \mathcal{R}$, such that the total CAPEX of the planned FON can be reduced as much as possible. Specifically,

Algorithm 1: AG-based Heuristic for FON Planning

Input: Parameters of MILP, and constant $\mathcal{M}$.
Output: Total CAPEX of planned FON $\mathbb{C}$.

1 $U = \emptyset$, sort $\mathcal{R}$ in descending order of demand data-rates;
2 **for** *each demand* $r \in \mathcal{R}$ *in sorted order* **do**
3 $LP^{W}_{r} = LP^{B}_{r} = \emptyset$, $\mathcal{P} = \emptyset$;
4 calculate $\mathcal{M}$ paths that can route r and only spans in a single fiber tree;
5 sort the paths in ascending order of the number of links in their fiber trees and store them in $\mathcal{P}$;
6 **if** $|\mathcal{P}| = 1$ **then**
7 mark the path in $\mathcal{P}$ as working path of r and record its fiber tree k, $LP^{W}_{r} = \{s_r, d_r, b_r, k\}$;
8 **end**
9 **if** $|\mathcal{P}| \geq 2$ **then**
10 select the first path in $\mathcal{P}$ as working path of r and record its fiber tree k_1, $LP^{W}_{r} = \{s_r, d_r, b_r, k_1\}$;
11 select the first path in $\mathcal{P}$ as backup path of r and record its fiber tree k_2, $LP^{B}_{r} = \{s_r, d_r, b_r, k_2\}$;
12 **end**
13 insert LP^{W}_{r} and LP^{B}_{r} into U;
14 **end**
15 **for** *each pair of* u, v *with at least one path in* $\{P_k\}$ **do**
16 find fiber tree k with the smallest number of links n_k;
17 connect u and v in AG $\mathcal{G}$ by a link with weight n_k;
18 **end**
19 **for** *each demand* $r \in \mathcal{R}$ *in sorted order* **do**
20 **if** LP^{W}_{r} *is not set* **then**
21 calculate $\mathcal{M}$-shortest paths from s_r to d_r in $\mathcal{G}$;
22 **for** *each obtained path* $m \in [1, \mathcal{M}]$ **do**
23 $U' = U$, insert each LP (u, v) on path m into U' as $\{u, v, b_r, k\}$ (k is the fiber tree);
24 run *Algorithm* 2 with U' to get a cost C_m;
25 **end**
26 select path m^* with the smallest C_m as working path of r (LP^{W}_{r});
27 remove paths sharing link(s) with LP^{W}_{r} in $\{P_k\}$;
28 repeat *Lines* 15-18 to build AG $\mathcal{G}$;
29 repeat *Lines* 21-26 for backup path of r (LP^{B}_{r});
30 insert LP^{W}_{r} and LP^{B}_{r} into U;
31 **else**
32 **if** LP^{B}_{r} *is not set* **then**
33 repeat *Lines* 27-29 for LP^{B}_{r} of r;
34 insert LP^{B}_{r} into U;
35 **end**
36 **end**
37 **end**
38 run *Algorithm* 2 with U to finalize FON planning and get total CAPEX $\mathbb{C}$ of the planned FON;

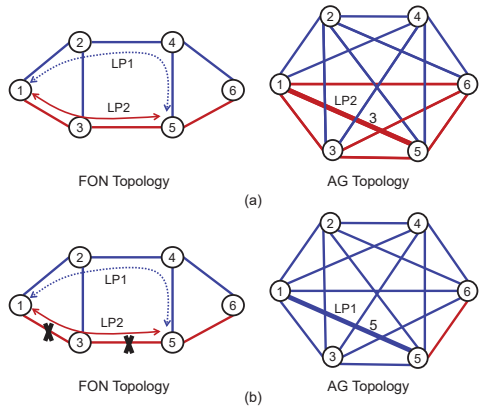

Fig. 4. Example on AG building for (a) Working LP and (b) Backup LP.

it tries to select a pair of link-disjoint paths whose fiber trees cover the smallest number of links as the working and backup LPs of each demand to reduce the possible usage of FS' and group the LPs of demands to save P2MP-TRXs. *Line* 1 is for the initialization. Then, the for-loop of *Lines* 2-14 checks each demand $r \in \mathcal{R}$ to set up its working and backup LPs (LP_r^W and LP_r^B) with the paths that only span in single fiber trees, in the best-effort way, and all the selected LPs are put in set U. Next, for each node pair u-v in V, we try to find a path in the overall path set $\{P_k, k \in [1, K]\}$, whose fiber tree contains the smallest number of links, and if such a path can be found, we connect u and v in AG $\mathcal{G}$ with a link whose weight is set as the number of links in the path's fiber tree (*Lines* 15-18).

Lines 19-37 find two link-disjoint paths for each demand whose working and backup LPs have not been determined yet, based on AG $\mathcal{G}$. Specifically, for each demand r, we check the $\mathcal{M}$-shortest paths from s_r to d_r in $\mathcal{G}$, include each of them as a potential working LP for r in set U', and apply *Algorithm* 2 to get the CAPEX of the FON planned with the LPs in U' (*Lines* 21-25). Here, each path in AG $\mathcal{G}$ is recorded as a series of tuple $\{u, v, b_r, k\}$, where (u, v) is an LP on the path, b_r is the data-rate of r, and k denotes the corresponding fiber tree that covers u and v in the physical topology $G(V, E)$. *Line* 26 selects the path that will lead to the smallest CAPEX as the working LP(s) of r (LP_r^W). We then remove the paths that share links with LP_r^W from the overall path set $\{P_k\}$, and repeat the procedure above to get the backup path of r (*Lines* 27-30). Similarly, *Lines* 32-35 obtain the backup path of r if its working path has already been determined. Finally, *Line* 38 runs *Algorithm* 2 with the selected LPs in U to get total CAPEX of the planned FON, and finishes the FON planning.

Fig. 4 shows an illustrative example on the AG construction in *Algorithm* 1. As shown in the left subplot of Fig. 4(a), the FON's physical topology consists of two fiber trees, marked in blue and red, respectively. Then, if we consider *Nodes* 1 and 5, two paths (*i.e.*, LP1 and LP2) can be found in the two fiber trees, respectively. As the fiber trees of LP1 and LP2 include 5 and 3 links, respectively, we build the AG in the right subplot of Fig. 4(a) with the information of LP2, *i.e.*, *Nodes* 1 and 5 are connected with a link whose weight is 3. By repeating this procedure, we can build the AG in Fig. 4(a), where the links in blue and red denote the LPs in the two corresponding fiber trees, respectively. Next, we assume that LP2 is included in the working LP of the demand. Therefore, all the links in LP2 are removed in the left subplot of Fig. 4(b). Then, in the AG built for determining the backup LP (shown in the right subplot of Fig. 4(b)), we can only consider LP1, *i.e.*, *Nodes* 1 and 5 are connected with a link whose weight is 5.

Algorithm 2: LP Grouping and Resource Assignment

Input: Set of LPs U, parameters of MILP.
Output: Total CAPEX $\mathcal{C}$, available P2MP-TRXs on nodes $\mathcal{T}$, P2MP-TRX assignments H^l.

1 $\mathcal{C} = 0$;
2 **while** $U \neq \emptyset$ **do**
3 select the node v with the largest data-rate to be assigned in U as a hub node;
4 move the LPs that use node v from U to N_v;
5 put the fiber trees that LPs in N_v are on in set $\mathcal{K}$;
6 **for** *each fiber tree* $k \in \mathcal{K}$ **do**
7 put LPs that are in N_v and use fiber tree k in set $\mathcal{N}_{v,k}$, and record their total data-rate as $b_{k,v}$;
8 **end**
9 sort $\mathcal{N}_{v,k}$ in descending order of $b_{k,v}$, and mark the $\mathcal{N}_{v,k}$ of each $k \in \mathcal{K}$ as unassigned;
10 **for** *each* $\mathcal{N}_{v,k}$ *in sorted order* **do**
11 **if** $\mathcal{N}_{v,k}$ *is unassigned* **then**
12 $C_o = \mathcal{C}' = 0$;
13 run *Algorithm* 3 with $\mathbb{N}_{v,k} = \mathcal{N}_{v,k}$ to assign P2MP-TRXs, SCs and FS' and get a cost C_o;
14 **for** *each* $\mathcal{N}_{v,k'}$ *after* $\mathcal{N}_{v,k}$ *in sorted order* **do**
15 **if** $\mathcal{N}_{v,k'}$ *is unassigned* **then**
16 $C'_o = C_{com} = 0$;
17 run *Algorithm* 3 with $\mathcal{N}_{v,k'}$ to get a cost C'_o;
18 $C_{sep} = C_o + C'_o$;
19 $\mathbb{N}'_v = \mathbb{N}_{v,k} \cup \mathcal{N}_{v,k'}$;
20 run *Algorithm* 3 with $\mathbb{N}'_v$ to get a cost C_{com};
21 **if** $C_{com} < C_{sep}$ **then**
22 $\mathcal{C}' = C_{com}$, $C_o = C_{com}$;
23 mark $\mathcal{N}_{v,k}$ and $\mathcal{N}_{v,k'}$ as assigned;
24 **else**
25 $\mathcal{C}' = C_o$;
26 mark $\mathcal{N}_{v,k}$ as assigned;
27 **end**
28 **end**
29 **end**
30 **end**
31 $\mathcal{C} = \mathcal{C} + \mathcal{C}'$;
32 **end**
33 run *Algorithm* 3 with all the $\{\mathcal{N}_{v,k}\}$ that are still unassigned to assign P2MP-TRXs, SCs and FS' and get a cost C', and update $\mathcal{C} = \mathcal{C} + C'$;
34 **end**

Algorithm 2 explains how to group a set of determined LPs in U to plan the FON with CAPEX as low as possible. In each iteration of the outer while-loop, we first select the node

Algorithm 3: Assigning P2MP-TRXs, SCs and FS'

Input: P2MP-TRXs on nodes $\mathcal{T}$ and their costs $\{C_t\}$, set(s) of LPs $\{u, v, b, k\}$.
Output: CAPEX C, P2MP-TRXs on nodes $\mathcal{T}$.

1 **for** $i \in \mathcal{T}$ **do**
2 $\quad w_i = C_i + \delta_i$, $v_i = T_i$;
3 **end**
4 apply Eqs. (21)-(23) to find the assignment of P2MP-TRXs $\mathcal{S}$ with the minimum possible cost;
5 sort P2MP-TRXs in $\mathcal{S}$ in descending order of their SCs;
6 $m' = b$;
7 **for** *each P2MP-TRX in* $\mathcal{S}$ *in sorted order* **do**
8 $\quad$ **if** $m' > 0$ **then**
9 $\quad\quad$ get number of SCs provided by the P2MP-TRX as m, $m^* = \min\{m, m'\}$;
10 $\quad\quad$ update CAPEX C based on C_i, m^* and k;
11 $\quad\quad$ update P2MP-TRX assignment in $\mathcal{T}$;
12 $\quad\quad$ $m' = m' - m^*$;
13 $\quad$ **end**
14 **end**

v with the largest data-rate to be assigned in U as the hub node for P2MP-TRX assignment, and then put the LPs that use v and their fiber trees in sets N_v and $\mathcal{K}$, respectively (*Lines* 3-5). *Lines* 6-9 group the LPs in N_v according to their fiber trees in sets $\{\mathcal{N}_{v,k}\}$, calculate the total data-rate that should be allocated on each fiber tree k to set up the LPs in $\mathcal{N}_{v,k}$, and sort the LP sets $\{\mathcal{N}_{v,k}\}$ accordingly. Next, the for-loop of *Lines* 10-32 checks the possible combinations of $\{\mathcal{N}_{v,k}, \mathcal{N}_{v,k'}\}$ to see whether provisioning the LPs in them together helps to reduce the total CAPEX, plans the FON accordingly, and marks the selected LP set(s) as assigned. Here, we use *Algorithm* 3 to assign P2MP-TRXs, SCs to P2MP-TRXs and FS' for establishing a set of LPs and obtain the corresponding CAPEX (*i.e.*, as in *Lines* 13, 17 and 20). Finally, *Line* 33 runs *Algorithm* 3 again to set up the LPs in all the $\{\mathcal{N}_{v,k}\}$ that are still unassigned and updates the total CAPEX. The aforementioned procedure is repeated until all the LPs in U have been established.

As for the actual assignments of P2MP-TRXs, SCs and FS', *Algorithm* 3 tries to find the most cost-efficient schemes. We treat the i-th P2MP-TRX as the i-th item, the possible cost of assigning the P2MP-TRX as the item's weight w_i, the number of SCs T_i that the P2MP-TRX can provide as the item's value v_i, and the required SCs b on a node as the expected value of a knapsack. Then, the problem of finding the most cost-efficient schemes becomes to obtain the minimum weight schemes that satisfy the value requirement (*i.e.*, b or more SCs are assigned on the node), which is a classical dual problem of the 0-1 knapsack problem and can be solved exactly with dynamic programming [41] (as shown in *Algorithm* 3). In *Algorithm* 3, *Lines* 1-3 are for the initialization. Then, *Line* 4 finds the P2MP-TRX assignment that leads to the minimum possible cost with dynamic programming, as follows.

First, to ensure that the assignment of P2MP-TRXs always leads to the least FS usage, we set $w_i = C_i + \delta_i$, where $\delta_i = 0$ if the leaf P2MP-TRX need to be assigned, otherwise,

$$\delta_i = \left\lceil \frac{4}{12.5} \cdot T_i \right\rceil \cdot \left(\frac{S \cdot n_k}{T_i} \right), \tag{21}$$

where T_i is the number of SCs provided by the i-th P2MP-TRX in $\mathcal{T}$, S is unit cost of FS usage in a fiber tree, and n_k is the number of links in the k-th fiber tree. Let $D(i, d)$ be the minimum required weight when we select the first i P2MP-TRXs with a total value of no less than d. Then, the initialization of the boundary condition and the state transition equation of the dynamic programming can be written as

$$D(0, d) = +\infty, \quad \forall d \in [0, b], \tag{22}$$

$$D(i+1, d) = \begin{cases} \min\left[D(i, d), w_{i+1}\right], & d \le v_{i+1}, \\ \min\left[D(i, d), D(i, d - v_{i+1}) + w_{i+1}\right], & d > v_{i+1}, \end{cases} \quad \forall i \in [0, |\mathcal{T}|),\ d \in [0, b]. \tag{23}$$

Finally, we prioritize assigning SCs to the P2MP-TRXs that provide more available SCs, and compute the assignments of P2MP-TRXs, SCs and FS' and the CAPEX C in *Lines* 5-14.

In addition to AG-LPG (*i.e.*, *Algorithm* 1), we also design a greedy-based benchmark (AG-GRD). *Algorithm* 4 shows its procedure. Specifically, it still uses the AG-based approach to calculate the working and backup LPs for each demand in R, but sets up the LPs one by one in a sorted order to reuse the assigned P2MP-TRXs to the maximum extent. *Lines* 1-6 are for the initialization, where we first build an AG for each demand r and then select two link-disjoint shortest paths in the AG as the working and backup LPs of r (*Lines* 2-4). *Lines* 5-6 combine the LPs that have the same source and destination and in a same fiber tree into an aggregated LP, and then sort the aggregated LPs to assist the subsequent P2MP-TRX and FS assignments. Next, the for-loop of *Lines* 7-29 set up the aggregated LPs in the sorted order. If an LP p is the first one, it does not have any assigned P2MP-TRXs to reuse, and thus we simply assign new P2MP-TRXs for it (*Lines* 9-10). Otherwise, *Lines* 12-27 try to set it up with the lowest additional CAPEX. Here, we try to establish p by 1) reusing the assigned P2MP-TRXs (*Lines* 13-20) and 2) assigning new P2MP-TRXs (*Lines* 21-22), and will select the scheme that causes lower additional CAPEX to actually set up p (*Lines* 23-27).

B. Complexity Analysis

The complexity of *Algorithm* 2 is $O(|V|^2 \cdot |K|^2 \cdot T \cdot \sum_r b_r)$. Hence, the complexity of *Algorithm* 1 is $O(|\mathcal{R}| \cdot \mathcal{M} \cdot |V|^2 \cdot |K|^2 \cdot T \cdot \sum_r b_r)$, which confirms that AG-LPG is in polynomial-time. The complexity of *Algorithm* 4 is $O(|E| \cdot |\mathcal{R}| \cdot |T| \cdot \sum_r b_r)$.

V. Numerical Simulations

In this section, we evaluate the performance of our proposed algorithms with numerical simulations.

A. Simulation Setup

In the simulations, we consider three topologies, which are a small-scale six-node topology and two realistic topologies (*i.e.*, the Italian Network (ITLNET) and German Network

Algorithm 4: Greedy-based Benchmark

Input: Parameters of MILP, and constant $\mathcal{M}$.
Output: CAPEX of planned FON $\mathbb{C}$, P2MP-TRXs on nodes $\mathcal{T}$, P2MP-TRX assignment H^l.

$\mathbb{C} = 0$;
for *each demand* $r \in \mathcal{R}$ **do**
  build an AG $\mathcal{G}$ and get two link-disjoint shortest paths in $\mathcal{G}$ as working and backup LPs of r to store in P';
end
combine LPs with same source, destination and in a same fiber tree into an "aggregated LP";
sort LPs in P' in descending order of their bit-rates;
for *each LP* $p \in P'$ *in sorted order* **do**
  if p *is the first LP* **then**
    assign two end nodes of p as hub and leaf nodes;
    assign P2MP-TRXs/SCs/FS' to p and update $\mathbb{C}$, $\mathcal{T}$ and H^l accordingly;
  else
    set the unassigned rate $\mathcal{B}$ of p as its data-rate;
    $\mathcal{B}' = \mathcal{B}$, $T_1 = \mathcal{T}$, $H_1^l = H^l$;
    while $\mathcal{B} > 0$ **do**
      if p *can reuse the assigned P2MP-TRXs* **then**
        get additional cost C_1 of reusing assigned P2MP-TRXs, and update $\mathcal{B}$ and H_1^l;
      else
        assign new P2MP-TRXs/SCs/FS' to p and update $\mathcal{B}$, C_1, T_1 and H_1^l accordinlgly;
      end
    end
    $T_2 = \mathcal{T}$, $H_2^l = H^l$;
    assign new P2MP-TRXs/SCs/FS' to p and update $\mathcal{B}'$, C_2, T_2 and H_2^l accordinlgly;
    if $C_1 < C_2$ **then**
      finalize setup of LP p as the scheme of $\{T_1, H_1^l\}$, and update $\mathcal{T}$, H^l and $\mathbb{C} = \mathbb{C} + C_1$;
    else
      finalize setup of LP p as the scheme of $\{T_2, H_2^l\}$, and update $\mathcal{T}$, H^l and $\mathbb{C} = \mathbb{C} + C_2$;
    end
  end
end

(GERNET) [23, 39]), as shown in Figs. 5(a)-5(c), respectively. We partition the six-node topology to get three fiber trees whose links are marked in red, blue and green. While for ITLNET and GERNET, fiber trees are obtained according to the study in [39] and different fiber tree links are marked with red and blue, respectively. The feasible capacities of P2MP-TRXs are $\{25, 100, 400\}$ Gbps, and each SC is assumed to use DP-16QAM at 4 GBaud and deliver a capacity of 25 Gbps [36]. Therefore, the numbers of SCs to realize capacities of $\{25, 100, 400\}$ Gbps are $\{1, 4, 16\}$, respectively, and their spectrum usages respectively become $\{1, 2, 6\}$ FS', each of which occupies 12.5 GHz. We set the unit costs of P2MP-TRXs at $\{25, 100, 400\}$ Gbps as $\{1, 2, 4\}$, respectively [36], while the unit cost of FS usage is assumed to be 0.03 based

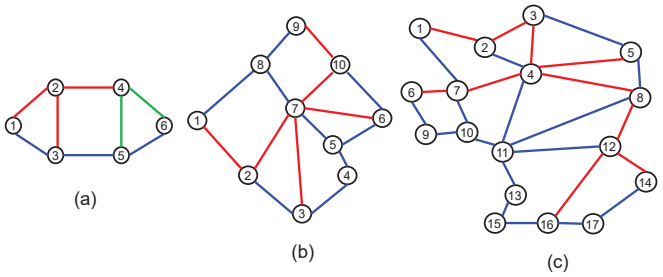

Fig. 5. Topologies used in simulations: (a) six-node topology (b) Italian Network, and (c) German Network (fiber trees are distinguished with colors).

on the practical setting in [42]. The number of P2MP-TRXs that can be deployed on each node (*i.e.*, T) and their types are set according to the actual traffic volume in each simulation. Each fiber link can accommodate 384 FS' at most [4].

The simulations compare four algorithms: 1) the one that solves the MILP in Section III-B directly (MILP), 2) *Algorithm* 1, which leverages AG and LP grouping (AG-LPG), 3) *Algorithm* 4, which is a greedy heuristic based on AG (AG-GRD), and 4) a heuristic that is modified from the approach [31] and realizes the protection design by building two link-disjoint fiber trees (TREE-PROT). The simulations are conducted on a computer with 2.2 GHz Intel Xeon Silver 4210 CPU and 128 GB memory, and the software environment is MATLAB 2020b with Gurobi 9.5.1 [43]. To ensure sufficient statistical accuracy, we average the results from 10 independent runs to get each data point in the simulations.

B. Small-Scale Simulations

We first conduct simulations with the six-node topology to compare the performance of MILP, AG-LPG and AG-GRD. Here, we set the longest running time of MILP to be 2 hours, and consider uniform traffic demands whose source and destination are randomly selected. As for each demand r, we make its data-rate uniformly distribute within $[25, 100]$ Gbps. If we denote the CAPEX of the FONs planned by MILP and a heuristic as $\mathbb{C}_{\text{MILP}}$ and $\mathbb{C}$, respectively, then the performance gap of the heuristic can be defined as

$$\xi = \frac{\mathbb{C} - \mathbb{C}_{\text{MILP}}}{\mathbb{C}_{\text{MILP}}}. \tag{24}$$

The simulation results are shown in Table I. We can see that MILP always provides the smallest CAPEX but it is also the most time-consuming, especially when dealing with relatively large FON planning instances. AG-LPG can always obtain near-optimal CAPEX with much shorter running time, achieving good trade-off between FON planning performance and running time. Specifically, the performance gap between MILP and AG-LPG is below 10.2% in Table I. Without LP grouping, AG-GRD performs much worse than MILP and AG-LPG, and the gap between MILP and AG-GRD ranges within $[14.26\%, 35.00\%]$, which is much larger than that of AG-LPG. This verifies the necessity of LP grouping in FON planning.

C. Large-Scale Simulations

We then compare the performance of AG-LPG and AG-GRD with the large-scale topologies in Figs. 5(b) and (c).

TABLE I
SIMULATION RESULTS WITH SIX-NODE TOPOLOGY

	MILP		AG-LPG			AG-GRD		
$\|\mathcal{R}\|$	CAPEX	Running Time (s)	CAPEX	Running Time (s)	Gap (%)	CAPEX	Running Time (s)	Gap (%)
6	37.32	51.71	41.12	0.07	10.18	48.96	0.06	31.19
8	45.14	134.39	47.14	0.07	4.43	60.96	0.08	35.00
10	54.14	2076.13	57.28	0.10	5.80	61.86	0.09	14.26
12	57.40	4421.80	61.20	0.18	6.62	71.26	0.11	24.15

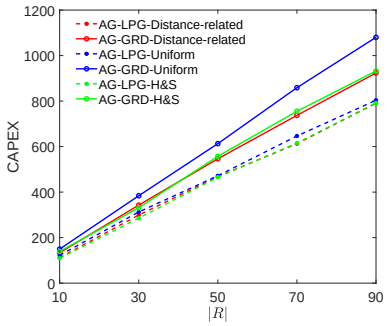

Fig. 6. CAPEX with ITLNET and different traffic patterns ($S = 0.03$).

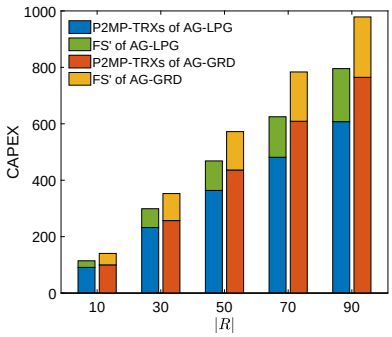

Fig. 7. Cost components in CAPEX with ITLNET ($S = 0.03$).

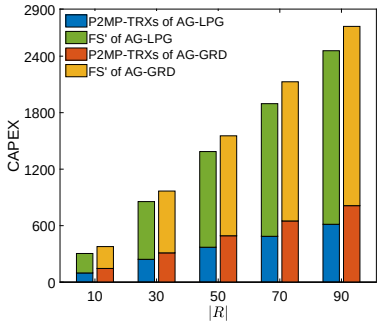

Fig. 8. Cost components in CAPEX with ITLNET ($S = 0.3$).

This time, we consider two unit costs of FS usage (*i.e.*, $S \in \{0.03, 0.3\}$), where $S = 0.3$ is for the scenario in which spectrum resources are limited. In addition to the uniform traffic pattern, the demands are also generated according to two more patterns: 1) distance-related demands where the amount of traffic between a source-destination pair is inversely proportional to the hop-count of the shortest path between the source and destination, and 2) H&S demands, with data-rates uniformly distributed within $[25, 200]$ Gbps.

Figs. 6-8 show the results of CAPEX from the simulations with ITLNET and three traffic patterns, when S is set as 0.03 and 0.3. Fig. 6 compares the results of CAPEX with $S = 0.03$ and various traffic patterns, and we can see that AG-LPG always outperforms AG-GRD to provide FONs with less CAPEX. To show the breakdown of cost components in CAPEX, Figs. 7 and 8 show the costs of P2MP-TRXs and FS usage in CAPEX, for the scenarios with S as 0.03 and 0.3, respectively, where the results are the averages of those with the three traffic patterns. Fig. 8 confirms that AG-LPG still outperforms AG-GRD when we have $S = 0.3$. Meanwhile, it is interesting to notice that the performance gap between AG-LPG and AG-GRD actually decreases when the unit cost of FS usage increases from 0.03 to 0.3. This is because the LP grouping in AG-LPG mainly helps to reduce the number of used P2MP-TRXs in the planned FON, and thus when the unit cost of FS usage increases, the corresponding advantage on CAPEX saving can become less significant. The results from the simulations with GERNET are illustrated in Figs. 9-11, where similar trends can be seen (*i.e.*, AG-LPG still outperforms AG-GRD in all the simulation scenarios). Hence, the effectiveness of our proposal is further confirmed.

In Figs. 7-8 and 10-11, we can also see that when we increase S from 0.03 to 0.3, the total FS usage contributes more to the total CAPEX, especially in GERNET (as shown in Figs. 10 and 11). This is because the broadcast-and-select nature of FON amplifies the impact of used FS' on CAPEX. Moreover, as there are more fiber links in each fiber tree in GERNET, more FS' will be used by an LP in the fiber tree, further increasing the cost of used FS'.

Finally, we compare AG-LPG with an existing algorithm for survivable FON planning (*i.e.*, the TREE-PROT in [31]) to further analyze its performance. However, as TREE-PROT needs to first determine the locations of hub and leaf nodes of P2MP-TRXs and then build two link-disjoint fiber trees for carrying working and backup traffic, we have to change the simulation scenario to adapt to it. Specifically, we select the six-node topology with three fiber trees and GERNET topology with two fiber trees, and choose hub and leaf nodes in them as shown in Fig. 12. In Fig. 12(a), the hub and leaf nodes are *Nodes* 4 (in yellow) and $\{2, 5, 6\}$ (in green), respectively.

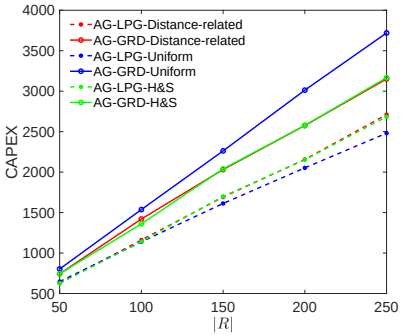

Fig. 9. CAPEX with GERNET and different traffic patterns ($S = 0.03$).

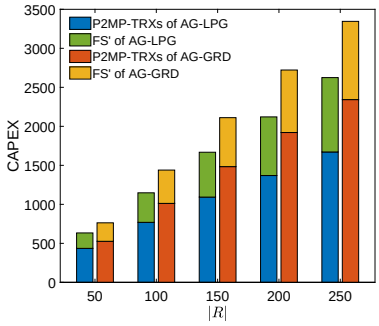

Fig. 10. Cost components in CAPEX with GERNET ($S = 0.03$).

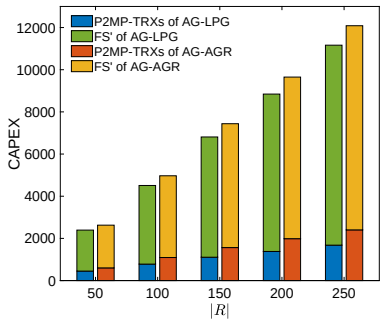

Fig. 11. Cost components in CAPEX with GERNET ($S = 0.3$).

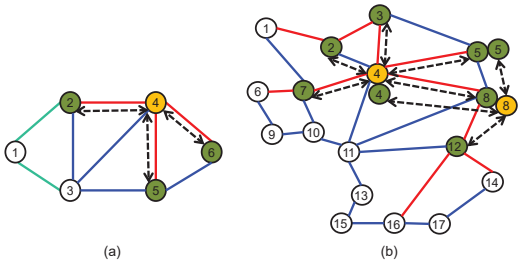

Fig. 12. Fiber trees in topologies for comparing AG-LPG and TREE-PROT.

In Fig. 12(b), there are two sets of hub-leaf nodes, where the hub nodes are *Nodes* 4 and 8, and their leaf nodes are *Nodes* $\{2, 3, 5, 7, 8\}$ and $\{4, 5, 12\}$, respectively.

Then, the simulations vary the data-rates required by the leaf nodes within $[25, 200]$ Gbps, average the CAPEX of 10 FONs planned by AG-LPG and TREE-PROT, and plot the results in Figs. 13 and 14. Here, we plot the results on CAPEX when the unit cost FS usage is set as $S \in \{0.03, 0.3\}$. We can see that the FONs planned by our AG-LPG are always more cost-efficient than those by TREE-PROT. However, we also observe that the cost of FS usage from AG-LPG is either comparable with or even higher than that from TREE-PROT. This is because TREE-PROT sets up link-disjoint working and backup fiber trees for each set of hub-leaf nodes, and thus all the working and backup LPs will be separately routed in single fiber trees. This actually helps to reduce FS usage. On the other hand, AG-LPG enables LP grouping and allows a hub P2MP-TRX to connect to leaf P2MP-TRXs in different fiber trees, which helps to save P2MP-TRXs, but the trade-off is that LPs can go across multiple fiber trees, leading to more FS usage. Note that, as we only consider one or two sets of hub-leaf nodes, the benefit of LP grouping in AG-LPG gets restricted. Nevertheless, in such scenarios, AG-LPG outperforms TREE-PROT, which further verifies the effectiveness of our proposal.

VI. Conclusion

In this paper, we studied the problem of survivable multilayer planning of FONs with P2MP-TRXs, which involves the joint optimization of the routing of working and backup LPs of traffic demands, and the allocation of P2MP-TRXs, the assignment of SCs to P2MP-TRXs, and the spectrum assignment on fiber trees for setting up the LPs. We first formulated an MILP model to solve the problem exactly, and then proposed a heuristic that leverages AG and LP grouping to improve the time-efficiency of problem-solving. Extensive simulations confirmed that our proposals can plan FONs with P2MP-TRXs cost-efficiently and outperform the benchmarks in all the simulation scenarios.

References

[1] Z. Pan *et al.*, "Advanced optical-label routing system supporting multicast, optical TTL, and multimedia applications," *J. Lightw. Technol.*, vol. 23, pp. 3270–3281, Oct. 2005.

[2] P. Lu *et al.*, "Highly-efficient data migration and backup for Big Data applications in elastic optical inter-datacenter networks," *IEEE Netw.*, vol. 29, pp. 36–42, Sept./Oct. 2015.

[3] V. Dukic *et al.*, "Beyond the mega-data center: networking multi-data center regions," in *Proc. of ACM SIGCOMM 2020*, pp. 765–781, Aug. 2020.

[4] Z. Zhu, W. Lu, L. Zhang, and N. Ansari, "Dynamic service provisioning in elastic optical networks with hybrid single-/multi-path routing," *J. Lightw. Technol.*, vol. 31, pp. 15–22, Jan. 2013.

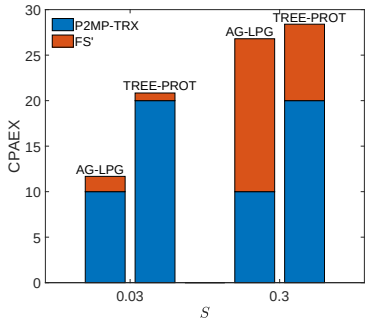

Fig. 13. Comparison of AG-LPG and TREE-PROT with six-node topology.

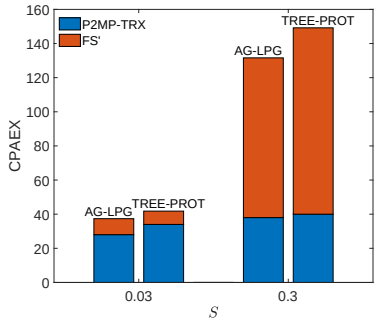

Fig. 14. Comparison of AG-LPG and TREE-PROT with GERNET.

[5] L. Gong *et al.*, "Efficient resource allocation for all-optical multicasting over spectrum-sliced elastic optical networks," *J. Opt. Commun. Netw.*, vol. 5, pp. 836–847, Aug. 2013.

[6] W. Shi, Z. Zhu, M. Zhang, and N. Ansari, "On the effect of bandwidth fragmentation on blocking probability in elastic optical networks," *IEEE Trans. Commun.*, vol. 61, pp. 2970–2978, Jul. 2013.

[7] Y. Yin *et al.*, "Spectral and spatial 2D fragmentation-aware routing and spectrum assignment algorithms in elastic optical networks," *J. Opt. Commun. Netw.*, vol. 5, pp. A100–A106, Oct. 2013.

[8] C. Chen *et al.*, "Demonstrations of efficient online spectrum defragmentation in software-defined elastic optical networks," *J. Lightw. Technol.*, vol. 32, pp. 4701–4711, Dec. 2014.

[9] M. Ju, F. Zhou, S. Xiao, and Z. Zhu, "Power-efficient protection with directed p-cycles for asymmetric traffic in elastic optical networks," *J. Lightw. Technol.*, vol. 34, pp. 4053–4065, Sept. 2016.

[10] Z. Zhu *et al.*, "Impairment- and splitting-aware cloud-ready multicast provisioning in elastic optical networks," *IEEE/ACM Trans. Netw.*, vol. 25, pp. 1220–1234, Apr. 2017.

[11] S. Li, D. Hu, W. Fang, and Z. Zhu, "Source routing with protocol-oblivious forwarding (POF) to enable efficient e-health data transfers," in *Proc. of ICC 2016*, pp. 1–6, Jun. 2016.

[12] K. Wu, P. Lu, and Z. Zhu, "Distributed online scheduling and routing of multicast-oriented tasks for profit-driven cloud computing," *IEEE Commun. Lett.*, vol. 20, pp. 684–687, Apr. 2016.

[13] J. Back *et al.*, "A filterless design with point-to-multipoint transceivers for cost-effective and challenging metro/regional aggregation topologies," in *Proc. of ONDM 2022*, pp. 1–6, May 2022.

[14] D. Welch *et al.*, "Point-to-multipoint optical networks using coherent digital subcarriers," *J. Lightw. Technol.*, vol. 39, pp. 5232–5247, Aug. 2021.

[15] Y. Zhang, M. O'Sullivan, and R. Hui, "Digital subcarrier multiplexing for flexible spectral allocation in optical transport network," *Opt. Express*, vol. 19, pp. 21 880–21 889, Oct. 2011.

[16] D. Krause *et al.*, "Design considerations for a digital subcarrier coherent optical modem," in *Proc. of OFC 2017*, pp. 1–3, Mar. 2017.

[17] C. Tremblay *et al.*, "Filterless optical networks: a unique and novel passive WAN network solution," in *Proc. of OECC/IOOC 2007*, pp. 466–467, Jul. 2007.

[18] O. Ayoub *et al.*, "Tutorial on filterless optical networks," *J. Opt. Commun. Netw.*, vol. 14, pp. 1–15, Mar. 2022.

[19] O. Karandin, O. Ayoub, F. Musumeci, and M. Tornatore, "A techno-economic comparison of filterless and wavelength-switched optical metro networks," in *Proc. of ICTON 2020*, pp. 1–4, Jul. 2020.

[20] P. Pavon-Marino *et al.*, "Technoeconomic impact of filterless data plane and agile control plane in the 5G optical metro," *J. Lightw. Technol.*, vol. 38, pp. 3801–3814, Aug. 2020.

[21] ——, "On the benefits of point-to-multipoint coherent optics for multi-layer capacity planning in ring networks with varying traffic profiles," *J. Opt. Commun. Netw.*, vol. 14, pp. B30–B44, May 2022.

[22] Q. Lv and Z. Zhu, "Planning security-aware filterless optical networks," in *Proc. of ACP 2021*, pp. 1–3, Oct. 2021.

[23] E. Archambault *et al.*, "Design and simulation of filterless optical networks: Problem definition and performance evaluation," *J. Opt. Commun. Netw.*, vol. 2, pp. 496–501, Aug. 2010.

[24] ——, "Routing and spectrum assignment in elastic filterless optical networks," *IEEE/ACM Trans. Netw.*, vol. 24, pp. 3578–3592, Dec. 2016.

[25] B. Jaumard, Y. Wang, and N. Huin, "Optimal design of filterless optical networks," in *Proc. of ICTON 2018*, pp. 1–5, Jul. 2018.

[26] R. Govindan *et al.*, "Evolve or die: High-availability design principles drawn from Google's network infrastructure," in *Proc. of ACM SIGCOMM 2016*, pp. 58–72, Aug. 2016.

[27] L. Gong and Z. Zhu, "Virtual optical network embedding (VONE) over elastic optical networks," *J. Lightw. Technol.*, vol. 32, pp. 450–460, Feb. 2014.

[28] Q. Sun, P. Lu, W. Lu, and Z. Zhu, "Forecast-assisted NFV service chain deployment based on affiliation-aware vNF placement," in *Proc. of GLOBECOM 2016*, pp. 1–6, Dec. 2016.

[29] J. Liu *et al.*, "On dynamic service function chain deployment and readjustment," *IEEE Trans. Netw. Serv. Manag.*, vol. 14, pp. 543–553, Sept. 2017.

[30] J. Yin *et al.*, "Experimental demonstration of building and operating QoS-aware survivable vSD-EONs with transparent resiliency," *Opt. Express*, vol. 25, pp. 15 468–15 480, 2017.

[31] M. Hosseini *et al.*, "Optimization of survivable filterless optical networks exploiting digital subcarrier multiplexing," *J. Opt. Commun. Netw.*, vol. 14, pp. 586–594, Jul. 2022.

[32] A. Rashidinejad *et al.*, "Real-time demonstration of 2.4Tbps (200Gbps/λ) bidirectional coherent DWDM-PON enabled by coherent nyquist subcarriers," in *Proc. of OFC 2020*, pp. 1–3, Mar. 2020.

[33] A. Napoli *et al.*, "Live network demonstration of point-to-multipoint coherent transmission for 5G mobile transport over existing fiber plant," in *Proc. of ECOC 2021*, pp. 1–4, Sept. 2021.

[34] J. Back *et al.*, "CAPEX savings enabled by point-to-multipoint coherent pluggable optics using digital subcarrier multiplexing in metro aggregation networks," in *Proc. of ECOC 2020*, pp. 1–4, Sept. 2020.

[35] M. Hosseini *et al.*, "Long-term cost-effectiveness of metro networks exploiting point-to-multipoint transceivers," in *Proc. of ONDM 2022*, pp. 1–6, May 2022.

[36] ——, "Optimized physical design of metro aggregation networks using point to multipoint transceivers," in *Proc. of OFC 2022*, pp. 1–3, Mar. 2022.

[37] G. Mantelet *et al.*, "Establishment of dynamic lightpaths in filterless optical networks," *J. Opt. Commun. Netw.*, vol. 5, pp. 1057–1065, Sept. 2013.

[38] Z. Xu *et al.*, "Flexible bandwidth allocation in filterless optical networks," *IEEE Commun. Lett.*, vol. 19, pp. 565–568, Apr. 2015.

[39] ——, "1+1 dedicated optical-layer protection strategy for filterless optical networks," *IEEE Commun. Lett.*, vol. 18, pp. 98–101, Jan. 2014.

[40] M. Hosseini *et al.*, "Optimized design of metro-aggregation networks exploiting digital subcarrier routing," in *Proc. of ACP 2021*, pp. 1–3, Oct. 2021.

[41] S. Martello, D. Pisinger, and P. Toth, "New trends in exact algorithms for the 0-1 knapsack problem," *Eur. J. Oper. Res.*, vol. 123, no. 2, pp. 325–332, 2000.

[42] V. Dukic *et al.*, "Beyond the mega-data center: networking multi-data center regions," in *Proc. of ACM SIGCOMM 2020*, pp. 765–781, Aug. 2020.

[43] "Gurobi." [Online]. Available: https://www.gurobi.com/.